Geometries and thermodynamic stability of $[Mo_3Se_{13}^{2-}]$@TM (TM = Sc-Ni) clusters: A theoretical investigation

Nguyen Thi Mai[1*], Phung Thi Thu[2], Ngo Thi Lan[3], Nguyen Thanh Tung[1]

[1]Institute of Materials Science, Vietnam Academy of Science and Technology, 18 Hoang Quoc Viet, Cau Giay, Hanoi, Vietnam;
[2]University of Science and Technology of Hanoi, Vietnam Academy of Science and Technology, 18 Hoang Quoc Viet, Cau Giay, Hanoi, Vietnam;
[3]Institute of Science and Technology, TNU - University of Sciences, Tan Thinh, Thai Nguyen City, Thai Nguyen, Vietnam.
[*]Corresponding author: maint@ims.vast.ac.vn
Received 5 Oct. 2024; Revised 18 Dec. 2024; Accepted 5 Feb. 2025; Published 25 Feb. 2025.
DOI: https://doi.org/10.54939/1859-1043.j.mst.101.2025.110-116

ABSTRACT

We study the geometric structure and thermodynamic stability of $[Mo_3Se_{13}]^{2-}$@TM atomic clusters (TM = Sc, Ti, V, Cr, Mn, Fe, Co and Ni) using the B3LYP/LanL2DZ level within the density functional theory. The presence of transition metal in the $[Mo_3Se_{13}]^{2-}$ clusters enhances the mobility of (Se-Se) terminals. Transition metal atoms preferentially attach to the sites, which forms the maximum number of bonds with Se atoms. Dissociation energy and entropy gradient analysis points out the $[Mo_3Se_{13}]^{2-}$@TM clusters favor to dissociate along two channels to create either Se-TM atoms or molecules. The $[Mo_3Se_{13}]^{2-}$@Ti, $[Mo_3Se_{13}]^{2-}$@Cr và $[Mo_3Se_{13}]^{2-}$@Ni can be predicted to be clusters with great catalytic potential due to high stability and minimum energy of 1.91, 1.57 and 1.78 eV, respectively.

Keywords: Atomic cluster; $[Mo_3Se_{13}]^{2-}$@TM; Thermodynamic stability; Dissociation energy; Entropy gradient.

1. INTRODUCTION

In parallel with the demand for renewable energy, water electrolysis technology produced hydrogen has been considered a green, clean and useful solution [1, 2]. This technology is a process composing of two half reactions: hydrogen evolution reaction (HER) and oxygen evolution reaction (OER). Nevertheless, the kinetics often occur sluggishly, leading to great limitations in large-scale production. To overcome this bottleneck, effective catalysts are a key factor in order to accelerate the reactions. Among the most potential catalyst, Pt metal and its derivatives have been brought out the highest HER performance. Being worth mentioning that their scarcity and expensiveness have made them utterly difficult to meet high volume mass H_2 production, effective alternatives are a priority strategy in this regard [3, 4].

Transition metal chalcogenides such as niobium disulfide crystals [5], tantalum disulfide crystals [5], amorphous molybdenum sulfide [6-8], crystalline molybdenum disulfide [9-11], amorphous molybdenum selenide [12, 13], crystalline molybdenum diselenide [14-16] and their composites with carbon-based materials [17-21] have been promising the alternatives with superior catalytic capabilities. Recently, scientists have successfully synthesized amorphous molybdenum selenide by refluxing $Mo(CO)_6$ and Se precursors in dichlorobenzene [12]. The prepared molybdenum selenide indicated an interesting catalytic performance of HER and its stability in water with a wide range of pH conditions, involving in alkaline solutions. Lewis and co-workers demonstrated the possibility of enhancing the catalytic activity of electrochemically treated amorphous molybdenum selenide, for example by repeating some potential polarization in a pH0 electrolyte solution [22]. Density functional theory (DFT) calculations have demonstrated the effectiveness in evaluating the hydrogen adsorption ability of doped metal clusters. Noticeably, the adsorption and dissociation of molecular hydrogen on the surface of transition metal (TM) doped $[Mo_3S_{13}]^{2-}$ atomic clusters were recently investigated using the DFT

calculations [23]. Research results show that the TM atoms form stably atomic bonds with S atoms, preserving the geometric structure of the pure cluster. The identified preferred adsorption sites are influenced by various factors, such as relative electronegativity, coordination number, and charge of the TM atom. In addition, the presence of these TM atoms significantly improved the hydrogen adsorption activity. The dissociation of a hydrogen molecule on $[Mo_3S_{13}]^{2-}$@TM clusters (TM = Sc, Cr, Mn, Fe, Co and Ni) is thermodynamically and kinetically favorable. A structure similar to the $[Mo_3S_{13}]^{2-}$ cluster, $[Mo_3Se_{13}]^{2-}$ cluster promises to have a high catalytic efficiency, which needs to be further studied and clarified.

In this study, we investigated the geometric structure and physical properties of $[Mo_3Se_{13}]^{2-}$ clusters doped with TM atoms (TM = Sc–Ni). A thorough analysis of the lowest energy structure, kinetic stability of these atomic clusters was performed. Our DFT results pointed out that the introduction of TM dopants can significantly change the stability of $[Mo_3Se_{13}]^{2-}$ clusters, and serve as a fundamental for further studies on hydrogen adsorption reactivity on $[Mo_3Se_{13}]^{2-}$@TM clusters.

2. METHOD

The quantum chemical calculation method DFT was chosen to study the structure and properties of $[Mo_3Se_{13}]^{2-}$@TM atomic clusters [10]. We used Gaussian package version 09 [24] with the support of Gaussview. The geometric structures of $[Mo_3Se_{13}]^{2-}$@TM clusters were optimized with the B3LYP/LanL2DZ. The choice of the B3LYP functional was based on previous studies on Mo–Se clusters [25]. The reliability and accuracy of the calculations were considered by evaluating the binding energy of TM-Se dimers using different functionals (B3LYP, B3P86, B3PW91 and PBEPBE) combined with LanL2DZ and SDD basis sets. The results were compared with available experimental results and summarized in table 1. The calculated binding energy of TM-Se using the B3LYP/LanL2DZ was in good agreement with the experimental values.

3. RESULTS AND DISCUSSION

3.1. Optimal geometric structure of $[Mo_3Se_{13}]^{2-}$@TM (TM = Sc-Ni)

Table 1. *Comparison table of functions/basis sets.*

Functional	Basis set	E_b (eV)							
		Sc-Se	Ti-Se	V-Se	Cr-Se	Mn-Se	Fe-Se	Co-Se	Ni-Se
B3LYP	LanL2DZ	3.97	3.90	3.34	2.34	2.10	3.07	1.65	3.22
	SDD	3.95	4.13	3.49	2.49	2.20	3.27	2.23	2.61
B3P86	LanL2DZ	4.23	4.01	3.58	2.40	3.78	3.20	2.56	2.75
	SDD	4.33	4.28	3.62	2.55	2.60	3.41	2.37	4.45
B3PW91	LanL2DZ	1.76	3.82	3.29	2.23	2.58	3.08	1.70	2.59
	SDD	4.23	4.09	3.43	2.37	2.50	3.31	1.90	2.69
PBEPBE	LanL2DZ	2.97	4.50	4.03	2.70	3.32	4.43	3.84	3.52
	SDD	4.75	4.70	4.12	2.84	3.15	3.36	5.72	3.53
		3.99 ± 0.18 [26]	3.95 ± 0.43 [26]	3.60 ± 0.22 [26]		2.08 [27]	2.74 [27]		3.22 [27]

The stable geometric structures of $[Mo_3Se_{13}]^{2-}$@TM clusters are determined as follows: Firstly, Gaussview package was used to construct all feasible geometric structures and then work as initial input data. After optimization, the oscillation frequencies or IR spectra were calculated. Next, a transition metal (TM = Sc-Ni) atom was attached into possible positions of the most stable structure of $[Mo_3Se_{13}]^{2-}$ (Fig. 1) to build $[Mo_3Se_{13}]^{2-}$@TM (TM = Sc-Ni) clusters. Finally,

the structural optimization steps were carried out like the $[Mo_3Se_{13}]^{2-}$ using the DFT method with the B3LYP function combined with the LANL2DZ basis set.

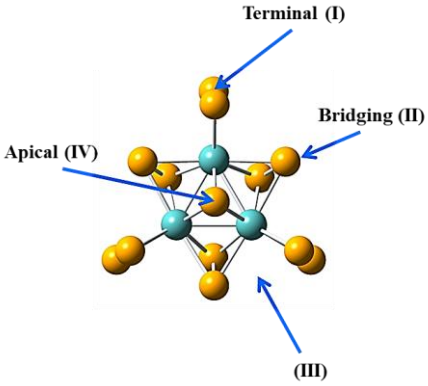

Figure 1. *Feasible locations for attaching transition metal atoms into the* $[Mo_3Se_{13}]^{2-}$.

In our calculations, a variety of geometric and spin isomers satisfy the convergence condition. Nevertheless, only the isomers with the lowest energy and no imaginal frequency were investigated and analyzed. Figure 2 depicts the optimized structures of $[Mo_3Se_{13}]^{2-}$, $[Mo_3Se_{13}]^{2-}$@TM.

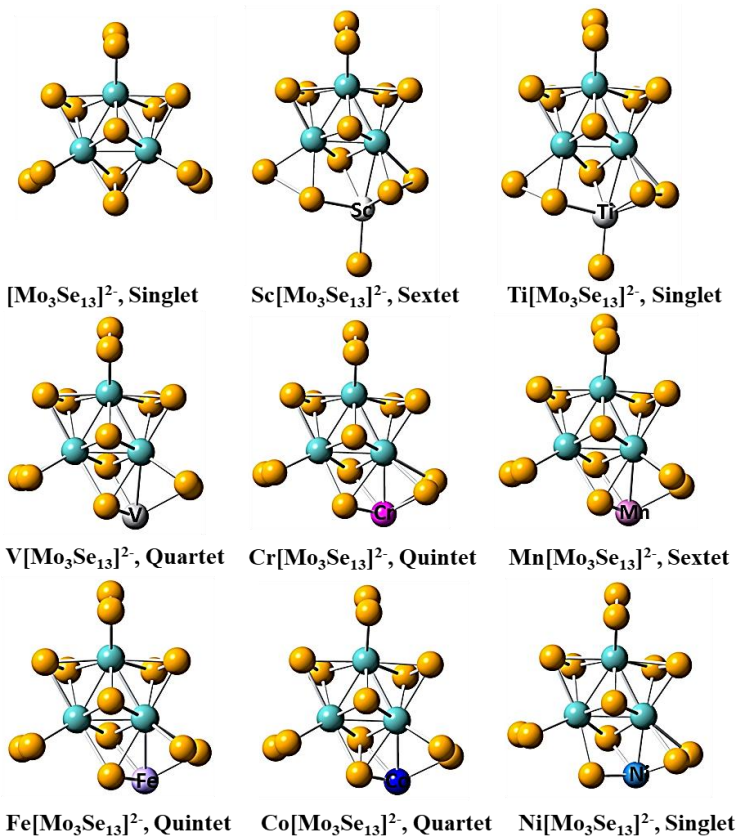

Figure 2. *Lowest-energy configurations of pure* $[Mo_3Se_{13}]^{2-}$ *and* $TM[Mo_3Se_{13}]^{2-}$ *(TM = Sc, Ti, V, Cr, Mn, Fe, Co, and Ni) clusters. Turquoise and yellow spheres denote Mo and Se respectively. Light gray, gray, dark gray, pink, violet, slate blue, blue, and royal blue spheres represent Sc, Ti, V, Cr, Mn, Fe, Co, and Ni, respectively.*

For the $[Mo_3Se_{13}]^{2-}$@Sc and $[Mo_3Se_{13}]^{2-}$@Ti clusters, their ground-states have similar structures. The most stable structure is determined by means of forming the maximum bonds between Sc/Ti atoms and Se atoms and slightly deforming the symmetrical structure of the pure counterpart. When doping Sc atom, the Se-Se bond length of bridging diselenide increases significantly (from 2.47 Å to 4.67 Å). In the presence of Ti atom, the Se-Se bond length of diselenide bridging also increases from 2.47 Å to 4.02 Å while pulling the diselenide terminal pair closer to the Se side.

In $[Mo_3Se_{13}]^{2-}$@TM (TM = V, Cr, Mn, Fe, Co and Ni) clusters, it found that their most stable structures are analogous in geometry. The TM atoms favor to localize at the (II) position, between the terminal and bridging diselenide. In addition, the introduce of TM = V, Cr, Mn, Fe, Co and Ni negligibly distorts the initial framework of $[Mo_3Se_{13}]^{2-}$ cluster, yet the Se-Se bond length of bridging diselenide increases from 2.47 Å to 2.98 Å; 2.76 Å; 2.83 Å; 2.85 Å; 3.02 Å and 3.16 Å corresponding to $[Mo_3Se_{13}]^{2-}$@V, $[Mo_3Se_{13}]^{2-}$@Cr, $[Mo_3Se_{13}]^{2-}$@Mn, $[Mo_3Se_{13}]^{2-}$@Fe, $[Mo_3Se_{13}]^{2-}$@Co and $[Mo_3Se_{13}]^{2-}$@Ni clusters.

From the geometric characteristics described above, it can be seen the rule of changing the geometric structure of the $[Mo_3Se_{13}]^{2-}$@TM cluster. The TM atoms preferentially attach to the diselenide bridging sites of the $[Mo_3Se_{13}]^{2-}$ cluster with the aim of generating maximum coordination number and forming rigid Se-TM-Se bridging bonds. In the case of doping light elements at the top of the 3D series, such as Sc and Ti, the distortion in the structure is observed, notably the Se-Se bond length of the Se_2^- bridging is significantly stretched. Both Sc and Ti atoms prefer to anchor in the inner central position to bind maximally with Se atoms, while doping V, Cr, Mn, Fe, Co and Ni atoms causes negligible deformations in the geometric structure.

3.2. Relative stability in $[Mo_3Se_{13}]^{2-}$@TM (TM = Sc-Ni) clusters

To study the relative stability of $[Mo_3Se_{13}]^{2-}$@TM clusters, we calculate the dissociation energy and entropy gradient. The DE is defined by the difference between the total electronic energy of daughter clusters and the electronic energy of the mother cluster. From the equilibrium theory, it is predicted that the evaporation rate constant depends strongly on the dissociation energy, and the decay channels with the lowest dissociation energy are the least stable.

The different decay channels of $[Mo_3Se_{13}]^{2-}$@TM discussed in this work include:

(1) $[Mo_3Se_{13}]^{2-}$@TM → $[Mo_3Se_{13}]^{2-}$ + TM

(2) $[Mo_3Se_{13}]^{2-}$@TM → $[Mo_3Se_{12}]^{2-}$@TM + Se

(3) $[Mo_3Se_{13}]^{2-}$@TM → $[Mo_3Se_{12}]^{2-}$ + Se-TM

Figure 3 shows the DE of $[Mo_3Se_{13}]^{2-}$@TM (TM = Sc-Ni) clusters with three channels, as mentioned above. The $[Mo_3Se_{13}]^{2-}$@TM (TM = Sc-Ni) tends to dissociate a Se atom to form $[Mo_3Se_{12}]^{2-}$@TM clusters, which is the most energetically preferred dissociation channel. The $[Mo_3Se_{13}]^{2-}$@V has the lowest DE, only requiring a small activation energy of 0.44 eV. Consequently, it can be facile to produce $[Mo_3Se_{12}]^{2-}$@V and one Se atom. The $[Mo_3Se_{13}]^{2-}$@Ti, $[Mo_3Se_{13}]^{2-}$@Cr and $[Mo_3Se_{13}]^{2-}$@Ni have higher stability, and the minimum energy required for the most preferential decay channel, which forms a Se atom and $[Mo_3Se_{12}]^{2-}$@TM cluster is 1.91, 1.57 and 1.78 eV, respectively. Simultaneously, from the general analysis and assessment of the DE in different dissociation directions, the energy required to separate a TM atom from the $[Mo_3Se_{13}]^{2-}$@TM is relatively large, typically the $[Mo_3Se_{13}]^{2-}$@Sc and $[Mo_3Se_{13}]^{2-}$@Ti. This result is completely consistent with the calculation of the energy of Se-TM bonds (TM = Sc-Ni). In the $[Mo_3Se_{13}]^{2-}$@Sc and $[Mo_3Se_{13}]^{2-}$@Ti, the binding energy between Se and Sc/Ti is relatively high (3.97 and 3.90 eV, respectively, calculated according to the B3LYP/LanL2DZ theoretical level). Therefore, the minimum energy for Sc and Ti loss is 5.56 and 6.75 eV,

respectively. These results are intimately linked to the geometric structure characteristics of $[Mo_3Se_{13}]^{2-}$@Sc and $[Mo_3Se_{13}]^{2-}$@Ti clusters. As mentioned above, in the presence of Sc/Ti atom, the Se-Se bond length of the bridging diselenide increases and the diselenide terminal pair is closer to Se, leading to increasing the stability of Se-Sc and Se-Ti bonds.

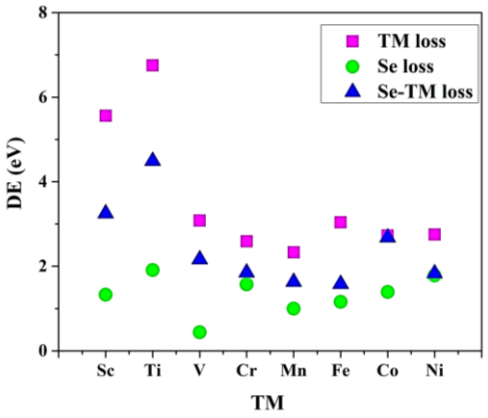

Figure 3. *The dissociation energy of $[Mo_3Se_{13}]^{2-}$@TM (TM = Sc-Ni) clusters as per dissociable channels.*

Calculation of Gibbs free energy for $[Mo_3Se_{13}]^{2-}$@TM (TM = Sc-Ni) clusters

Table 2. *Entropy gradient ΔS per temperature unit (eV/K) in the evaporation reaction of an atom or a molecule from the $[Mo_3Se_{13}]^{2-}$@TM (TM = Sc-Ni) clusters.*

Cluster	TM loss	Se loss	Se-TM loss
$[Mo_3Se_{13}]^{2-}$@Sc	0.0006805	0.001281	0.002579
$[Mo_3Se_{13}]^{2-}$@Ti	0.0013482	0.001415	0.001884
$[Mo_3Se_{13}]^{2-}$@V	0.0013184	0.001454	0.001859
$[Mo_3Se_{13}]^{2-}$@Cr	0.0012535	0.001398	0.001832
$[Mo_3Se_{13}]^{2-}$@Mn	0.0012179	0.001495	0.001795
$[Mo_3Se_{13}]^{2-}$@Fe	0.0011558	0.001423	0.001728
$[Mo_3Se_{13}]^{2-}$@Co	0.0012241	0.001443	0.001792
$[Mo_3Se_{13}]^{2-}$@Ni	0.0013849	0.001390	0.001951
Average	0.001198	0.001413	0.001927

In the case of two dissociation channels with nearly equal dissociation energy, it is necessary to consider the thermodynamic value of entropy S. To determine the thermodynamic stability as well as more preciseness of the most favorable dissociation channel, we proceed to calculate the entropy gradient ΔS, and find out the entropy in relation to the internal energy of the atomic cluster.

$-T\Delta S_{bind}$ parameter of decay reaction: $[Mo_3Se_{13}]^{2-}$@TM → Se + $[Mo_3Se_{12}]^{2-}$@TM is calculated following to the formula below:

$$-T\Delta S_{\text{bind}} = -TS([Mo_3Se_{13}]^{2-}@TM) - \left(-TS([Mo_3Se_{12}]^{2-}@TM)\right) - (-TS(Se))$$

We first calculate the ΔS of $[Mo_3Se_{13}]^{2-}$@TM according to three dissociation channels mentioned above. From table 2, the increase in entropy following dissociation channels that evaporate a Se-TM molecule is larger than that of channels that evaporate a TM atom or a Se atom. Fundamentally, the dissociation process leading to the evaporation of diatomic molecules will cause greater disorder (vibration, translational vibration, rotational vibration) than dissociation channels that only there is evaporation of an atom. Consequently, a larger and more

dominant change in entropy occurs. These findings are in good agreement with the discussion above. Particularly, at the same temperature, the Se-TM molecular dissociation channels have a higher thermodynamic increase than single metal atom dissociation channels (a TM or a Se atom). Therefore, it needs to provide the same energy to activate the decay reaction into the Se-TM molecules or the Se atoms, then the channel that dissociates into Se-TM molecules will be given priority kinetically because it has a larger thermodynamic entropy gradient.

4. CONCLUSIONS

This work used a quantum computing method based on the density functional theory to investigate the stable geometric structure of $[Mo_3Se_{13}]^{2-}$@TM atomic clusters. The results reveal that 3d transition metal atoms preferentially dope into position (III) between the terminal and bridging diselenide. The transition metal atoms in $[Mo_3Se_{13}]^{2-}$@TM clusters contribute to increasing the mobility of (Se-Se) terminal sites. Additionally, they participate in the formation of maximum bonds with Se atoms. By the B3LYP/LanL2DZ function/basis set, we determined thermodynamic parameters, including dissociation energy and entropy gradient ΔS for the $[Mo_3Se_{13}]^{2-}$@TM clusters via the different dissociation directions. It is found that producing Se / TM atoms or Se-TM molecules is the most preferential dissociation channel. Among the studied clusters, the $[Mo_3Se_{13}]^{2-}$@Ti, $[Mo_3Se_{13}]^{2-}$@Cr, and $[Mo_3Se_{13}]^{2-}$@Ni have higher stability with minimal energy required to separate a Se atom is 1.91, 1.57, and 1.78 eV, respectively. Conversely, the $[Mo_3Se_{13}]^{2-}$@V cluster is the least stable, with an energy of 0.44 eV.

Acknowledgement: *The authors thank the Vietnam Academy of Science and Technology for the financial support under grant No. TĐHYD0.04/22-24*

REFERENCES

[1]. Lewis NS *et al, "Powering the planet: chemical challenges in solar energy utilization"* Proc Natl Acad Sci USA **103,** 15729e35, **(**2006).
[2]. Walter MG *et al, "Solar water splitting cells"* Chem Rev **110**, 6446e73, **(**2010).
[3]. Roger I *et al, "Earth-abundant catalysts for electrochemical and photoelectrochemical water splitting"* Nat Rev Chem **1**, 0003, (2017).
[4]. McKone JR *et al,* "*Earth-abundant hydrogen evolution electrocatalysts"* Chem Sci **5**, 865e78, (2014).
[5]. Liu Y *et al, "Self-optimizing, highly surfaceactive layered metal dichalcogenide catalysts for hydrogen evolution"* Nat Energy **2**, 17127, (2017).
[6]. Tran PD *et al, "Coordination polymer structure and revisited hydrogen evolution catalytic mechanism for amorphous molybdenum sulfide"* Nat Mater **15**, 640e6, (2016).
[7]. Merki D *et al, "Amorphous molybdenum sulfide films as catalysts for electrochemical hydrogen production in water"* Chem Sci **2**, 1262e7, (2011).
[8]. Benck JD *et al, "Amorphous molybdenum sulfide catalysts for electrochemical hydrogen production: insights into the Origin of their catalytic activity"* ACS Catal **2**, 1916e23, (2012).
[9]. Ding Q *et al*, "*Efficient electrocatalytic and photoelectrochemical hydrogen generation using MoS_2 and related compounds"* Chem 1, 699e726, (2016).
[10]. Benck JD *et al, "Catalyzing the hydrogen evolution reaction (HER) with molybdenum sulfide nanomaterials"* ACS Catal **4**, 3957e71, (2014).
[11]. Voiry D *et al, "Low-dimensional catalysts for hydrogen evolution and CO_2 reduction"* Nat Rev Chem **2**, 0105, (2018).
[12]. Nguyen QT *et al, "Novel amorphous molybdenum selenide as an efficient catalyst for hydrogen evolution reaction"* ACS Appl Mater Interfaces **10**, 8659e65, (2018).
[13]. Chia X, Pumera M. *"Inverse opal-like porous MoSex films for hydrogen evolution catalysis: overpotential-pore size dependence"* ACS Appl Mater Interfaces **10**, 4937e45, (2018).
[14]. Gao D *et al, "Dual-native vacancy activated basal plane and conductivity of $MoSe_2$ with high-efficiency hydrogen evolution reaction"* Small **14**, 1704150, (2018).
[15]. Jian C, Cai Q, Hong W, Li J, Liu W. *"Edge-riched $MoSe_2/MoO_2$ hybrid electrocatalyst for efficient hydrogen evolution reaction"* Small **14**, 1703798, (2018).

[16]. Ren X, Ma Q, Ren P, Wang Y. "*Synthesis of nitrogen-doped $MoSe_2$ nanosheets with enhanced electrocatalytic activity for hydrogen evolution reaction*" Int J Hydrogen Energy **43**, 15275e80, (2018).
[17]. Ren X, Yao Y, Ren Y, Wang Y, Peng Y. *"Facile sol-gel synthesis of C@$MoSe_2$ core-shell composites as advanced hydrogen evolution reaction catalyst"* Mater Lett **238**, 286e9, **(**2019).
[18]. He HY, He Z, Shen Q. *"Effcient hydrogen evolution catalytic activity of graphene/metallic MoS_2 nanosheet heterostructures synthesized by a one-step hydrothermal process"* Int J Hydrogen Energy **43**, 21835e43, (2018).
[19]. Liu Y *et al, "Exfoliated MoS_2 with porous graphene nanosheets for enhanced electrochemical hydrogen evolution"* Int J Hydrogen Energy **43**, 13946e52, (2018).
[20]. Xu L *et al, "Boosting electrocatalytic activity of ultrathin $MoSe_2$/C composites for hydrogen evolution via a surfactant assisted hydrothermal method"* Int J Hydrogen Energy **43**, 15749e61, (2018).
[21]. Han X, Tong X, Liu X, Chen A, Wen X, Yang N, Guo XY. "*Hydrogen evolution reaction on hybrid catalysts of vertical MoS_2 nanosheets and hydrogenated graphene"* ACS Catal **8**, 1828e36, (2018).
[22]. Saadi FH *et al, "Operando synthesis of macroporous molybdenum diselenide films for electrocatalysis of the hydrogen-evolution reaction"* ACS Catal **4**, 2866e73, (2014).
[23]. Thu Thi Phung *et al, "Unraveling Hydrogen Adsorption on Transition Metal-Doped $[Mo_3S_{13}]^{2-}$ Clusters: Insights from Density Functional Theory Calculations"* ACS Omega **9**, 20467, (2024).
[24]. M. J. Frisch, et al., Gaussian 09, Revision B. 01. Gaussian, Inc., Wallingford., (2009).
[25]. Chuc T. Nguyen *et al, "Structure and electrochemical property of amorphous molybdenum selenide H_2-evolving catalysts prepared by a solvothermal synthesis"* J. Hydrogen Energy **44**, 13273, (2019).
[26]. J. Shee et al. J. Chem. Theory Comput. **15**, 2346, (2019).
[27]. https://labs.chem.ucsb.edu

TÓM TẮT

Cấu trúc hình học và độ bền nhiệt động của cụm nguyên tử $[Mo_3Se_{13}]^{2-}$@TM (TM = Sc-Ni): Một nghiên cứu lý thuyết

Trong nghiên cứu này, chúng tôi xác định cấu trúc hình học và độ bền nhiệt động lực học của các cụm nguyên tử nano $[Mo_3Se_{13}]^{2-}$@TM (TM = Sc, Ti, V, Cr, Mn, Fe, Co và Ni) dựa trên phương pháp phiếm hàm mật độ với mức lý thuyết B3LYP/LanL2DZ. Kết quả bước đầu cho thấy sự có mặt của các nguyên tử kim loại chuyển tiếp trong các cụm nguyên tử nano $[Mo_3Se_{13}]^{2-}$ làm tăng độ linh động của các vị trí $(Se\text{-}Se)_{terminal}$. Các nguyên tử kim loại chuyển tiếp ưu tiên gắn vào vị trí tạo tối đa số liên kết với các nguyên tử Se. Kết quả phân tích năng lượng phân ly và biến thiên entropy cho thấy cụm $[Mo_3Se_{13}]^{2-}$@TM ưu tiên phân ly dọc theo hai kênh tạo ra các nguyên tử hoặc phân tử Se-TM. Trong số các cụm được nghiên cứu, $[Mo_3Se_{13}]^{2-}$@Ti, $[Mo_3Se_{13}]^{2-}$@Cr và $[Mo_3Se_{13}]^{2-}$@Ni có độ ổn định cao hơn và năng lượng tối thiểu cần thiết để phân ly một nguyên tử Se tương ứng là 1,91, 1,57 và 1,78 eV.

Từ khoá: Phiếm hàm mật độ; Kim loại chuyển tiếp.